Adsorption of CO2 on Amine-Functionalized Y-Type Zeolites

ARTICLE *in* ENERGY & FUELS · JANUARY 2010

Impact Factor: 2.79 · DOI: 10.1021/ef901077k

4 AUTHORS, INCLUDING:

Fengsheng Su
Mingchi University of Technology
18 PUBLICATIONS **1,227** CITATIONS
SEE PROFILE

Chungsying Lu
National Chung Hsing University
107 PUBLICATIONS **3,148** CITATIONS
SEE PROFILE

Energy Fuels **2010,** *24,* 1441–1448 · DOI:10.1021/ef901077k
Published on Web 01/13/2010

energy&fuels
article

Adsorption of CO_2 on Amine-Functionalized Y-Type Zeolites

Fengsheng Su, Chungsying Lu,* Shih-Chun Kuo, and Wanting Zeng

Department of Environmental Engineering, National Chung Hsing University 250 Kuo Kuang Road, Taichung 402, Taiwan

Received September 22, 2009. Revised Manuscript Received December 21, 2009

Commercially available Y-type zeolite with a Si/Al molar ratio of 60 (abbreviated as Y60) was modified by tetraethylenepentamine (TEPA) to study their characterizations and adsorption/desorption properties of CO_2 from gas streams. The surface nature of Y60 was changed after TEPA modification, which causes a significant enhancement in CO_2 adsorption capacity. The CO_2 adsorption capacity of Y60(TEPA) increased with the temperature at 30−60 °C but decreased with the temperature at 60−70 °C. The mechanism of CO_2 adsorption on Y60 is entirely a physical interaction but becomes mainly attributable to a chemical interaction after TEPA modification. The CO_2 adsorption capacity of Y60(TEPA) was influenced by the presence of water vapor and reached as high as 4.27 mmol of CO_2/g of sorbent at a water vapor of 7%. The cyclic CO_2 adsorption showed that the adsorbed CO_2 could be desorbed from the surface of Y60(TEPA) at 75 °C for 4 h. The adsorption capacities and the physicochemical properties of Y60(TEPA) were preserved after 20 cycles of adsorption and regeneration, suggesting that the Y60(TEPA) can be stably employed in the prolonged cyclic operation and that they are possibly cost-effective sorbents for CO_2 capture from flue gas.

Introduction

The CO_2 capture and storage (CCS) technologies from flue gas are considered to be effective means to lessen the global warming issue after the Kyoto Protocol came into force on February 16, 2005. Various CO_2 capture technologies, including absorption, adsorption, cryogenics, membranes, etc., have been investigated.[1,2] Among them, the design of a full-scale adsorption process might be feasible and the development of a promising material that would efficiently adsorb CO_2 with high adsorption capacity and low energy penalty for the regeneration process will undoubtedly enhance the competitiveness of adsorptive separation in a flue gas application.[3] Possible dry sorbents documented in the literature include activated carbon,[4−6] carbon nanotubes,[6−9] X-type zeolite,[10−12] SBA-15 mesoporous silica sorbents,[13−16] mesoporous spherical-silica particles,[17,18] silica gel,[19,20] and mesoporous molecular sieve MCM-41.[21,22]

Although CO_2 adsorption on dry sorbents had been studied by the foregoing researchers, a higher CO_2 adsorption capacity (more than 2 mmol/g) is needed for practical applications in the field.[23] Because the Y-type zeolites possess a well-defined pore structure and their pore sizes are of the same magnitude as CO_2 molecules, they are therefore expected to have a good affinity for CO_2 capture.[24] However, such studies are still limited in the literature.

In this paper, the Y-type zeolite was modified with tetraethylenepentamine ($H_2NC_2H_4NHC_2H_4NHC_2H_4NHC_2H_4NH_2$, abbreviated as TEPA), which was found to greatly enhance CO_2 capture when supported on mesoporous silica[15] or high-molecular-weight polymetric compounds,[25] to investigate their physicochemical properties and adsorption/desorption behaviors

*To whom correspondence should be addressed. Fax: +886-4-2286-2587. E-mail: clu@nchu.edu.tw.

(1) White, C. M.; Strazisar, B. R.; Granite, E. J.; Hoffman, J. S.; Pennline, H. W. *J. Air Waste Manage. Assoc.* **2003**, *53* (6), 645–715.
(2) Aaron, D.; Tsouris, C. *Sep. Sci. Technol.* **2005**, *40* (1−3), 321–348.
(3) Intergovernmental Panel on Climate Change (IPCC). Special report on carbon dioxide capture and storage. http://www.ipcc.ch/activity/srccs/index.htm (accessed on Sept 2005).
(4) Siriwardane, R. V.; Shen, M. S.; Fisher, E. P.; Losch, J. *Energy Fuels* **2001**, *15* (2), 279–284.
(5) Prezepiórski, J.; Skrodzewicz, M.; Morawski, A. W. *Appl. Surf. Sci.* **2004**, *225* (1−4), 235–242.
(6) Lu, C.; Bai, H.; Wu, B.; Su, F.; Hwang, J. F. *Energy Fuels* **2008**, *22* (5), 3050–3056.
(7) Cinke, M.; Li, J.; Bauschlicher, C. W., Jr.; Ricca, A.; Meyyappan, M. *Chem. Phys. Lett.* **2003**, *376* (5−6), 761–766.
(8) Su, F.; Lu, C.; Chen, W.; Bai, H.; Hwang, J. F. *Sci. Total Environ.* **2009**, *407* (8), 3017–3023.
(9) Hsu, S.-C.; Lu, C.; Su, F.; Zeng, W.; Chen, W. *Chem. Eng. Sci.* **2010**, *65* (4), 1354−1361.
(10) Siriwardane, R. V.; Shen, M. S.; Fisher, E. P.; Poston, J. A. *Energy Fuels* **2005**, *19* (3), 1153–1159.
(11) Lee, J. S.; Kim, J. H.; Kim, J. T.; Suh, J. K.; Lee, J. M.; Lee, C. H. *J. Chem. Eng. Data* **2002**, *47* (5), 1237–1242.
(12) Chatti, R.; Bansiwal, A. K.; Thote, J. A.; Kumar, V.; Jadhav, P.; Lokhande, S. K.; Biniwale, R. B.; Labhsetwar, N. K.; Rayalu, S. S. *Microporous Mesoporous Mater.* **2009**, *121* (1−3), 84–89.
(13) Gray, M. L.; Soong, Y.; Champagne, K. J.; Pennline, H.; Baltrus, J. P.; Stevens, R. W., Jr.; Khatri, R.; Chuang, S. S. C.; Filburn, T. *Fuel Process. Technol.* **2005**, *86* (14−15), 1449–1455.
(14) Hiyoshi, N.; Yogo, K.; Yashima, T. *Microporous Mesoporous Mater.* **2005**, *84* (1−3), 357–365.
(15) Yue, M. B.; Chun, Y.; Cao, Y.; Dong, X.; Zhu, J. H. *Adv. Funct. Mater.* **2006**, *16* (13), 1717–1722.
(16) Wang, X.; Schwartz, V.; Clark, J. C.; Ma, X.; Overbury, S.; Xu, X.; Song, C. *J. Phys. Chem. C* **2009**, *113* (17), 7260–7268.
(17) Lu, C.; Su, F.; Hsu, S.; Chen, W.; Bai, H.; Hwang, J. F.; Lee, H. H. *Fuel Process. Technol.* **2009**, *90* (12), 1543–1549.
(18) Lu, C.; Bai, H.; Su, F.; Chen, W.; Hwang, J. F.; Lee, H. H. *J. Air Waste Manage. Assoc.* **2010**, in press.
(19) Huang, H. Y.; Yang, R. T.; Chinn, D.; Munson, C. L. *Ind. Eng. Chem. Res.* **2003**, *42* (12), 2427–2433.
(20) Knowles, G. P.; Delaney, S. W.; Chaffee, A. L. *Ind. Eng. Chem. Res.* **2006**, *45* (8), 2626–2633.
(21) Xu, X. C.; Song, C.; Andresen, J. M.; Miller, B. G.; Scaroni, A. W. *Energy Fuels* **2002**, *16* (6), 1463–1469.
(22) Xu, X. C.; Song, C. S.; Miller, B. G.; Scaroni, A. W. *Ind. Eng. Chem. Res.* **2005**, *44* (21), 8113–8119.
(23) Li, P.; Ge, B.; Zhang, S.; Chen, S.; Zhang, Q.; Zhao, Y. *Langmuir* **2008**, *24* (13), 6567–6574.
(24) Gao, W.; Butler, D.; Tomasko, D. L. *Langmuir* **2004**, *20* (19), 8083–8089.
(25) Schladt, M. J.; Filburn, T. P.; Helble, J. J. *Ind. Eng. Chem. Res.* **2007**, *46* (5), 1590–1597.

of CO_2 from gas streams. Effects of the temperature at 30−70 °C and water vapor at 0−17.4% on the CO_2 adsorption are also conducted and discussed.

Experimental Section

Preparation of the Sorbents. Commercially available Y-type zeolite with a Si/Al molar ratio of 60 (abbreviated as Y60) (Zeolyst International, Valley Forge, PA) was selected as the sorbent for CO_2 capture from gas streams. In a preliminary test, Y60 zeolite was found to have a higher CO_2 adsorption capacity than those with Si/Al molar ratios of 5.1, 30, or 80. The physical properties of Y60 indicated that surface area, pore volume, and average pore diameter of Y60 are 975.26 m^2/g, 0.305 cm^3/g, and 0.31 nm for micropores and 726.95 m^2/g, 0.344 cm^3/g, and 9.12 nm for mesopores, respectively. Most pore volumes of micro- and mesopores are located in 0.2−0.4 and 2−5 nm, respectively.

Raw Y60 (1 g) was dispersed into flasks containing TEPA solution (1 g of 99% TEPA + 10 g of ethanol). The TEPA−Y60 mixture was heated and stirred for 2 h. After the mixture was cooled to room temperature, it was filtered through a 0.45 μm fiber filter. The filtrated solid was then dehydrated at 100 °C for 2 h and dried at 80 °C by passing pure N_2 gas for 2 h. The weight of the final product [Y60(TEPA)] was about 2.0 g, indicating that the TEPA loading in the pores of Y60 is 50 wt %, which has been found to possess a higher adsorption capacity of 15% CO_2 at 60 °C than those with 20, 30, 40, and 60 wt % TEPA loading.

To compare the adsorption capacity of CO_2 on Y60 with other sorbents, commercially available granular activated carbon (abbreviated as GAC, BPL, Calgon Carbon Corporation, Tianjia, China) and mordenite zeolite (abbreviated as MZ, CBV21A, Zeolyst International, Valley Forge, PA) were chosen because of their wide use for the removal of volatile organic compounds from waste gases. They were also put through the same modification process as Y60.

Adsorption Experiments. The CO_2 adsorption experiments were conducted in a cylindrical Pyrex glass column, having a length of 16 cm and an internal diameter of 1.27 cm. The adsorption column was packed with 5.0 g of sorbents (packing height of 14 cm) and placed within a temperature-controlled oven. Because the best location for CO_2 adsorption in a coal-fired power plant to take place is after the flue gas desulfurization (FGD) and before the stack,[2] the tested temperature was selected from 30 to 70 °C (in 10 °C increments), which covers the typical temperature range of 45−55 °C in post-FGD. The water vapor of the gas stream was kept at 0% with the exception of during the moisture effect study, in which the water vapor range of 0−17.4% was evaluated at 60 °C. The selection of this water vapor range covers the typical water vapor range of 8−12% in flue gas.[26] In this case, moisture was introduced into the gas stream by dispersing 15% of CO_2 gas through a water bath.

Compressed air was passed first through a silica gel air dryer to remove moisture and oil and then through a HEPA filter (Gelman Science, Ann Arbor, MI) to remove particulates. Two mass flow controllers (MKS Instrument, Inc., Andover, MA) were employed to control the influent CO_2 concentration by regulating flow rates of clean air (diluting gas) and pure CO_2 (99.95%) entering the mixing chamber. The influent and effluent gas streams were flowed into a CO_2 analyzer for online measurement. All of the experiments are repeated 2 times, and only the mean values were reported.

The influent CO_2 concentration was in the range of 5−50%, which was selected to be representative of different CO_2 levels in combustion gases from many kinds of industrial activities, such as coal-fired power plants (12−14%), cement plants (14−33%),[27] or coal gasification systems (30−35%).[28] The inlet flow rate (Q_{in}) was controlled at 0.1 L/min, which is equivalent to an empty-bed retention time of 12.2 s. The CO_2 adsorption capacity (q, mg/g) at a certain time (t, min) was estimated as

$$q = \frac{1}{m}\int_0^t (Q_{in}C_{in} - Q_{eff}C_{eff})\mathrm{d}t \quad (1)$$

where m is the dry weight of virgin sorbents (g), Q_{eff} is the effluent gas flow rate (L/min), and C_{in} and C_{eff} are the influent and effluent CO_2 concentrations (mg/L), which are expressed in terms of percent in volume (%). The relationship between two units can be derived from the ideal gas law. Blank tests (without sorbents) were conducted with various C_{in}. The adsorption capacities of blanks were eliminated from the adsorption capacities of Y60 and Y60(TEPA).

Physisorption and Chemisorption. Most adsorption processes are a combination of the physical interaction (physisorption) and chemical interaction (chemisorption). A distinction of these two processes is very useful in understanding the factors that influence the rate of the adsorption process. The equilibrium capacities of CO_2 because of physisorption (q_{ep}) and chemisorption (q_{ec}) were estimated as follows.[29]

As the adsorption reached equilibrium, the weight of adsorbed CO_2 was measured and then the influent gas was changed from 15% CO_2 to N_2 gas and controlled at a Q_{sys} of 0.1 L/min. The outlet of the adsorption column was connected to a vacuum pump, which was operated at 0.145 bar. After the CO_2 level in the effluent gas streams was undetectable (~30 min), which reflects the completion of the desorption process, the remaining weight of spent sorbents was measured. The weight loss after vacuum desorption is attributed to q_{ep}, while the weight remaining after vacuum desorption is attributed to q_{ec}.

Adsorption/Desorption Experiments. The adsorption process was controlled at 60 °C and with a C_{in} of 15%. As the CO_2 adsorption on Y60(TEPA) reached equilibrium, the adsorption capacity (q_e) was measured. A combination of thermal desorption and vacuum desorption of CO_2 was used by changing influent gas to purified air, which was operated at the same flow rate as in the adsorption experiment and at 0.145 atm. The optimum temperature and time for regeneration of spent Y60(TEPA) were determined by laboratory testing. Cyclic CO_2 adsorption on Y60(TEPA) was conducted for 20 cycles of adsorption and regeneration.

Analytical Methods. The CO_2 concentration was determined using a CO_2 analyzer (Model 2820, Bacharach, Inc., U.K.). The physical properties of sorbents were determined by N_2 adsorption/desorption at 77 K via a Micromeritics ASAP 2020 volumetric sorption analyzer (Norcross, GA). N_2 adsorption/desorption isotherms were measured at a relative pressure (P_{N_2}/P_0) range of 0.0001−0.99 and then employed to determine surface area, pore volume, and average pore diameter via the Barrett−Johner−Halenda (BJH) equation for pore size of 1.7−100 nm and the micropore (MP) method for pore size below 1.7 nm. The crystal phase of sorbents was characterized by a powder X-ray diffractometer (XRD, Mac Science, Co. Ltd., Japan) using Cu Kα radiation (40 kV, 30 mA). The thermal stability of sorbents in air was determined by a thermogravimetric analyzer (TGA i1000, Instrument Specialists Incorporated, Twin Lakes, WI) at a heating rate of 10 °C/min at 30−800 °C. The surface functional groups of sorbents were evaluated by a Fourier transform infrared (FTIR) spectrometer (Spectrum 100 FTIR spectrometer, Perkin-Elmer, Waltham, MA). The water vapor in air stream was measured by a

(26) Chaffee, A. L.; Knowles, G. P.; Liang, Z.; Zhang, J.; Xiao, P.; Webley, P. A. *Int. J. Greenhouse Gas Control* **2007**, *1* (1), 11–18.

(27) Bosoaga, A.; Masek, O.; Oakey, J. E. *Energy Procedia* **2009**, *1* (1), 133–140.

(28) Cormos, C. C.; Starr, F.; Tzimas, E.; Peteves, S. *Int. J. Hydrogen Energy* **2008**, *33* (4), 1286–1294.

(29) Hsu, H.; Lu, C. *Sep. Sci. Technol.* **2007**, *42* (12), 2751–2766.

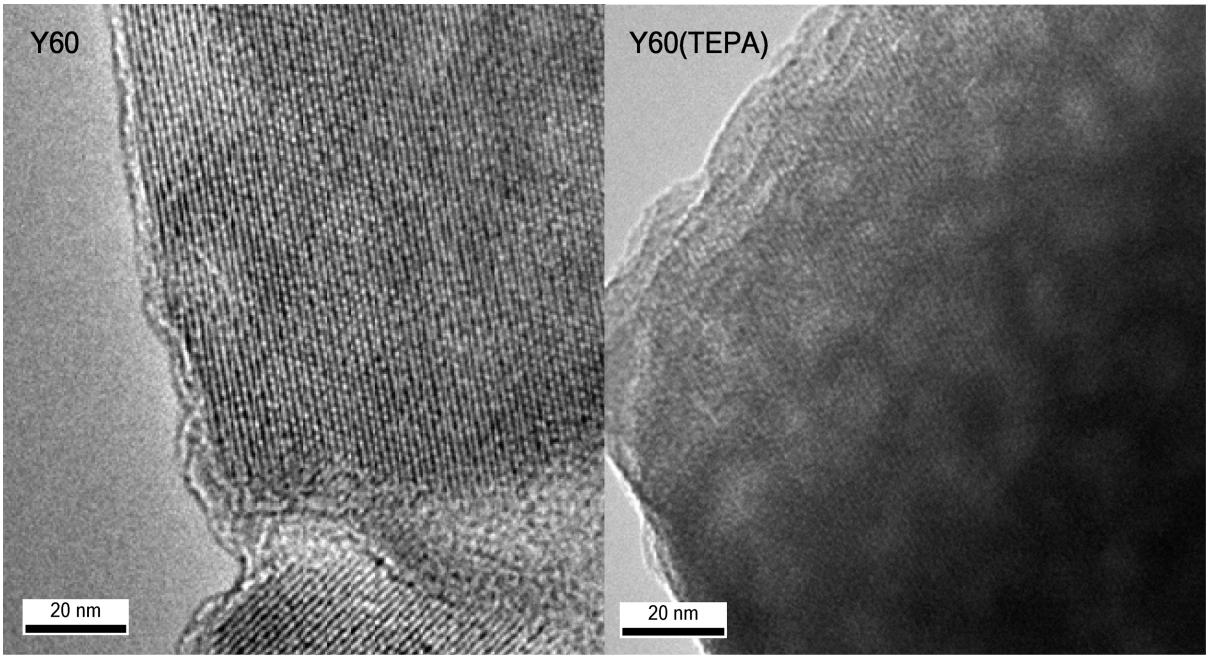

Figure 1. TEM images of Y60 and Y60(TEPA).

temperature/relative humidity sensor (Rotronic Hygromer M130D, Rotronic Co., Ltd., Zurich, Switzerland).

Results and Discussion

Characterizations of Y60 and Y60(TEPA). Figure 1 exhibits the transmission electron microscopy TEM images of Y60 and Y60(TEPA). It is apparent that both samples have micropores and channels of regular dimensions within the crystalline lattice. These microporous materials have periodic cavities and channels throughout the structure, with pore sizes of approximately 0.36 nm. The TEM image of Y60(TEPA) shows less obvious micropores and channels because of layers of TEPA grafted on their surface.

The XRD patterns of Y60 and Y60(TEPA) are displayed in Figure 2. It is seen that the (Si 210) diffraction peaks located at $2\theta = 6.0-6.5°$ are clearly observed for both samples, indicating evidence of a well-ordered hexagonal structure.[30] The intensity of the diffraction peak became weak after the TEPA modification, implying that the pore structure order is better for Y60.

Figure 3 reveals the TGA profiles and the corresponding differential thermogravimetry (DTG) profiles of Y60. It is obvious that the TGA profile of Y60 showed a weight loss close to 8.4% below 100 °C, which could be attributed to the evaporation of adsorbed water. As the temperature exceeded 100 °C, the weight loss became insignificant and a remaining weight of 89.8% was observed at 800 °C. The Y60(TEPA) had a broader temperature range for weight loss and exhibited four main weight loss regions. The first weight loss region (< 120 °C) is due to the evaporation of adsorbed water. The second region (120−200 °C) displayed a remarkable weight loss. As shown in the DTG profile, the maximum weight loss rate was observed at 186 °C, which can be mainly attributed to the Hofmann elimination of trimethylamine in Y60(TEPA).[31] The third

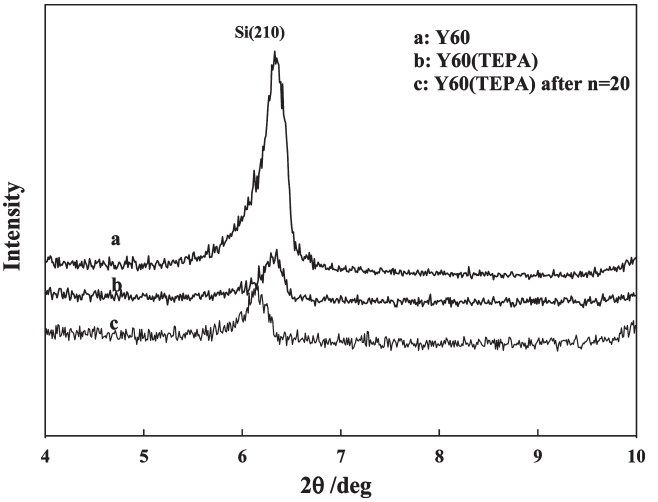

Figure 2. XRD patterns of Y60 and Y60(TEPA).

region (200−700 °C) showed a weight loss near 21.1% because of the carbon chain ($C-H_2$) decomposition accompanied by oxidation processes.[31] After temperature exceeded 700 °C, the weight loss became small (< 0.2%) and a remaining weight of 43.2% was obtained at 800 °C. The Y60(TEPA) demonstrated thermal stability in air up to 90 °C, suggesting that regeneration of spent Y60(TEPA) should be conducted at temperatures below 90 °C.

Figure 4 displays the IR spectra of Y60 and Y60(TEPA). It is observed that the IR spectrum of Y60 show significant bands at 3450, 1637, and 1080 cm^{-1}, which are related to O−H stretching vibrations of the hydrogen-bonded silanol groups, H−O−H bend, and Si−O−Si asymmetric stretching vibrations, respectively.[16,32] The IR spectrum of Y60(TEPA) exhibit significant bands at 3450, 3270, 2933, 2814, 1630, 1563, 1470, 1320, and 1080 cm^{-1}. The bands at 2933 and

(30) Bourlinos, A. B.; Karakassides, M. A.; Petridis, D. *J. Phys. Chem. B* **2000**, *104* (18), 4375–4380.
(31) Yue, M. B.; Sun, L. B.; Cao, Y.; Wang, Y.; Wang, Z. J.; Zhu, J. H. *Chem.—Eur. J.* **2008**, *14* (11), 3442–3451.
(32) Zheng, F.; Tran, D. N.; Busche, B. J.; Fryxell, G. E.; Addleman, R. S.; Zemanian, T. S.; Aardahl, C. L. *Ind. Eng. Chem. Res.* **2005**, *44* (9), 3099–3105.

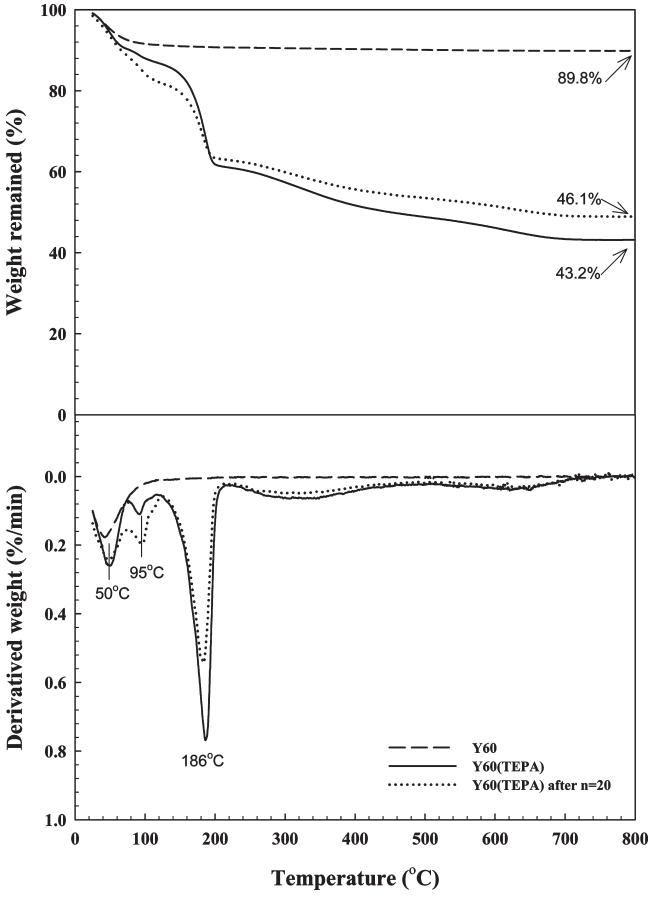

Figure 3. TGA and DTG profiles of Y60 and Y60(TEPA).

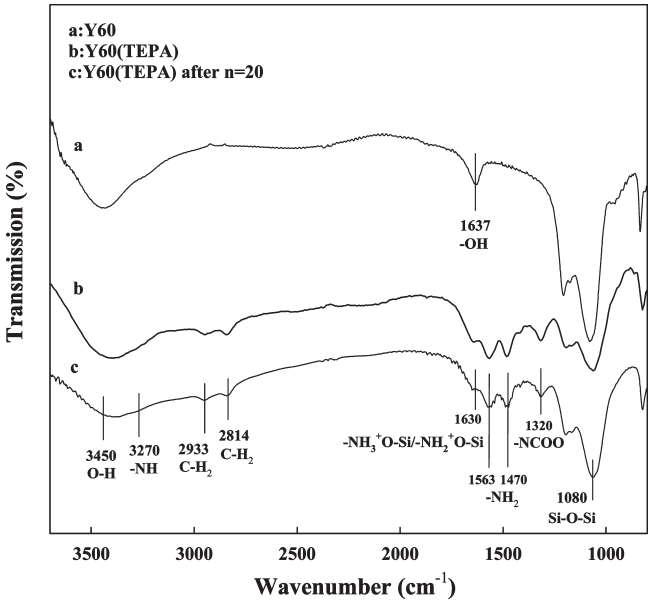

Figure 4. IR spectra of Y60 and Y60(TEPA).

2814 cm^{-1} can be assigned to C−H_2 stretching from $CH_2CH_2CH_2$−NH_2 groups, while the bands at 1563 and 1470 cm^{-1} can be related to N−H_2 vibration in the primary amine group (RNH_2).[16,33,34] The band at 3270 cm^{-1} can be related to N−H vibration in the secondary amine group (R_2NH). The band at 1630 cm^{-1} can be associated with the NH_3^+ deformation of the protonated primary amine group or secondary amine group (−NH_3^+O−Si/−NH_2^+O−Si), which is the product of the amine group interacted with the silanol group (Si−OH) on the Y60 surface.[16] The presence of C−H_2, N−H_2, N−H, and −NH_3^+O−Si/−NH_2^+O−Si and decreased O−H at 3450 cm^{-1} after the TEPA modification confirm that TEPA has been grafted on the surface of Y60. The band at 1320 cm^{-1} can be assigned to weakly adsorbed gaseous CO_2.[16,34]

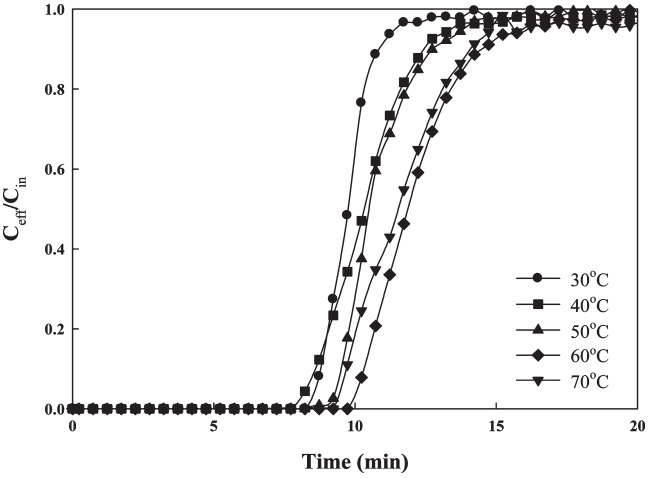

Figure 5. Breakthrough curves of 30% CO_2 adsorption on Y60-(TEPA) in 30−70 °C.

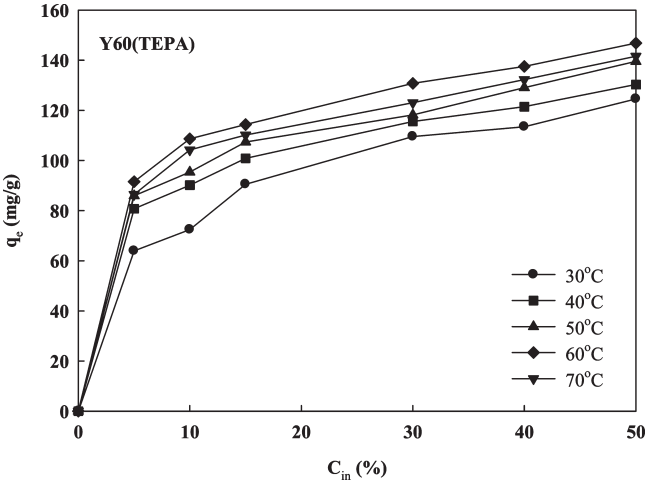

Figure 6. CO_2 adsorption isotherms of Y60(TEPA) at 30−70 °C.

Adsorption Behaviors. Figure 5 shows the breakthrough curves of 30% CO_2 adsorption on Y60(TEPA) in 30−70 °C. It is seen that initially the CO_2 can be completely adsorbed on Y60(TEPA) from air streams. The breakthrough time (the time at which the effluent CO_2 concentration reaches 10% allowable breakthrough concentration) follows the order of 60 > 70 > 50 > 30 > 40 °C.

Figure 6 shows the CO_2 adsorption isotherms of Y60-(TEPA) in 30−70 °C. It is apparent that the q_e increased with C_{in} and the temperature at 30−60 °C but slightly decreased with the temperature at 60−70 °C. Raising the temperature from 30 to 60 °C increased the molecular flexibility of TEPA loaded in the mesopore channels of Y60(TEPA), which may partly contribute to the increase of q_e at higher temperatures.[16] However, further raising the temperature to 70 °C

(33) Chang, A. C. C.; Chuang, S. S. C.; Gray, M.; Soong, Y. *Energy Fuels* **2003**, *17* (2), 468–473.
(34) Huang, H. Y.; Yang, R. T.; Chinn, D.; Munson, C. L. *Ind. Eng. Chem. Res.* **2003**, *42* (12), 2427–2433.

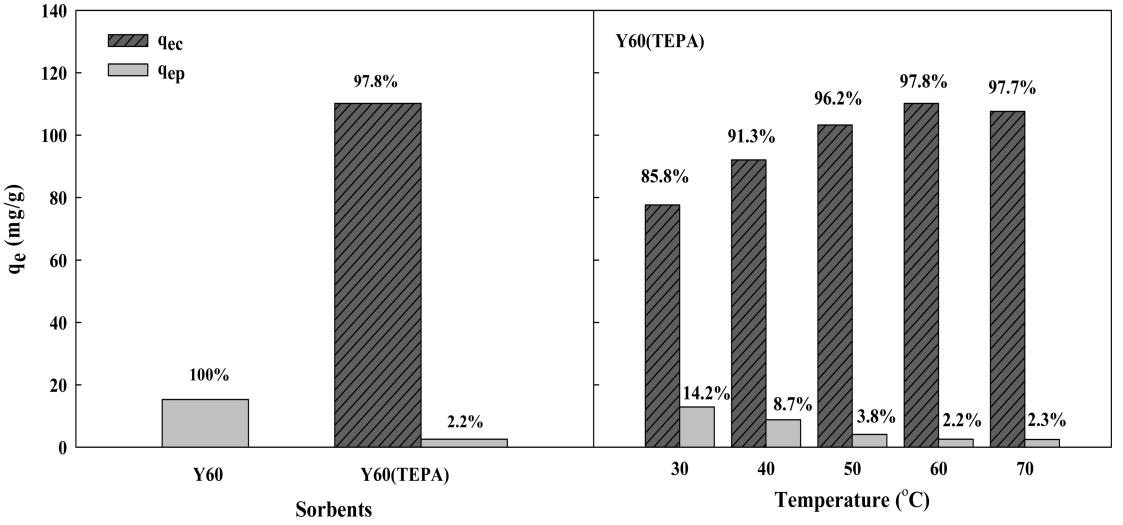

Figure 7. Physisorption and chemisorption capacities of 15% CO_2 on Y60(TEPA) at 30−70 °C.

led to the decrease of q_e likely because of the decrease of the chemical interaction and van der Waals' force between CO_2 molecules and the surface of Y60(TEPA). Similar observations on the correlation of q_e with temperature had been reported in other studies of amine-functionalized SBA-15[16] and MCM-41,[22,36] where the maximum q_e was found at 75 °C. This may be due to the nature of silica sorbents. The q_e at 30, 40, 50, 60, and 70 °C are, respectively, 90.5, 100.9, 107.4, 112.7, and 110.1 mg/g with a C_{in} of 15% and 124.5, 130.3, 139.5, 146.8, and 141.6 mg/g with a C_{in} of 50%. These values are all more than 2 mmol/g, reflecting that Y60-(TEPA) is an efficient CO_2 sorbent and possesses good potential for CO_2 capture from flue gas.

The q_{ec} and q_{ep} of Y60 and Y60(TEPA) with a C_{in} of 15% were subsequently evaluated, and the results are shown in Figure 7. Percentage ratios of q_{ec} and q_{ep} to q_e are also indicated in the top of each bar graph. It is seen that q_{ec} of Y60 greatly increased from 0 to 111.8 mg/g after the TEPA modification, indicating that the introduction of TEPA to the Y60 surface significantly improved the adsorption selectivity of CO_2 from gas streams. The q_{ec} of Y60(TEPA) increased from 77.7 to 111.8 mg/g as the temperature increased from 30 to 60 °C but slightly decreased to 107.6 mg/g as the temperature further increased to 70 °C, which are consistent with the changes in q_e of Y60(TEPA) with the temperature, as shown in Figure 6. The q_{ep} of Y60(TEPA) decreased with a rise in the temperature because of the decrease of van der Waals' force.

The percentage ratio of q_{ec} of Y60 is equal to 0, while percentage ratios of q_{ep} and q_{ec} of Y60(TEPA) were, respectively, in the range of 2.3−14.2 and 85.8−97.7%. This indicated that CO_2 adsorption on Y60 is entirely a physical interaction but became mainly attributable to a chemical interaction after the TEPA modification.

Figure 8 shows the q_e of 15% CO_2 adsorption on Y60-(TEPA) at 60 °C under various water vapors in air stream. It is observed that the q_e of Y60(TEPA) quickly increased from 112.7 to 189.9 mg/g (4.27 mmol/g) as the water vapor increased from 0 to 7% but slightly decreased from 189.9 to 161.59 mg/g as the water vapor further increased from 7 to 17.4%.

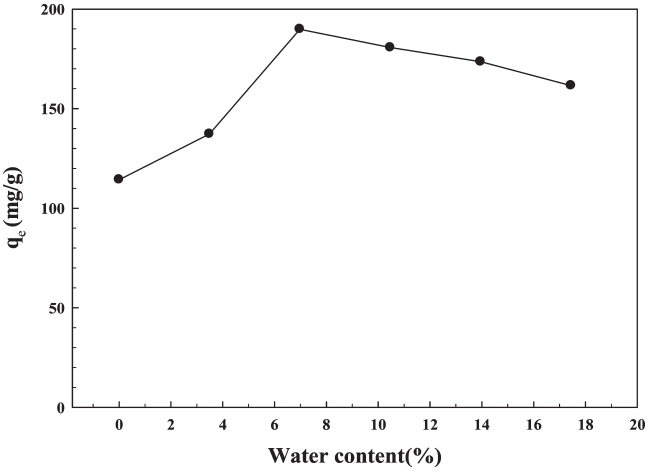

Figure 8. Effects of the water vapor on 15% CO_2 adsorption on Y60(TEPA) at 60 °C.

In the literature, the CO_2 adsorption capacity in moist stream may decrease if a hydrophilic material, such as 13X zeolite, is being used[37] or it may increase if a hydrophobic material, such as carbon nanotube (CNT), is being used.[8] Employed Y60-(TEPA) is a highly hydrophobic material compared to 13X zeolite; however, it still contains some −OH groups, as indicated in the IR spectrum (Figure 4), which make it slightly hydrophilic compared to the CNTs. Thus, there are two possible reasons to explain the increase in q_e in the presence of some amount of moisture. First, Y60(TEPA) contains primary amine (RNH_2) and secondary amine (R_2NH); both amines can react with CO_2 and lead to the formation of a carbamate ion by reactions 2 and 3. The presence of water then regenerates amine molecules by reactions 4 and 5.[16]

$$CO_2 + 2RNH_2 \leftrightarrow RNH_3^+ + RNHCOO^- \quad (2)$$

$$CO_2 + 2R_2NH \leftrightarrow R_2NH_2^+ + R_2NCOO^- \quad (3)$$

$$RNHCOO^- + H_2O \leftrightarrow RNH_2 + HCO_3^- \quad (4)$$

$$R_2NCOO^- + H_2O \leftrightarrow R_2NH + HCO_3^- \quad (5)$$

(35) Hicks, J. C.; Drese, J. H.; Fauth, D. J.; Gray, M. L.; Qi, G.; Jones, C. W. *J. Am. Chem. Soc.* **2008**, *130* (10), 2902–2903.
(36) Xu, X.; Song, C.; Andresen, J. M.; Miller, B. G.; Scaroni, A. W. *Microporous Mesoporous Mater.* **2003**, *62* (1−2), 29–45.
(37) Jadhav, P. D.; Chatti, R. V.; Biniwale, R. B.; Labhsetwar, N. K.; Devotta, S.; Rayalu, S. S. *Energy Fuels* **2007**, *21* (6), 3555–3559.

Table 1. Comparisons of q_e via Various Raw and Amine-Functionalized Silica Sorbents

sorbents	modification chemicals	q_e (mg/g)	conditions	references
Y60	TEPA	112.7	C_{in}, 15%; T, 60 °C	this work
		146.8	C_{in}, 50%; T, 60 °C	
MZ	TEPA	72.9	C_{in}, 15%; T, 60 °C	this work
SBA-15	APTS	88.5	C_{in}, 10%; T, 25 °C	13
SBA-15		2.2	C_{in}, 15%; T, 60 °C	14
	APTS	22.9		
	TA	69.5		
SBA-15	EDA	20	C_{in}, 15%; T, 25 °C	32
SBA-15	APTS	17.6	C_{in}, 4%; T, 25 °C	33
SBA-15	HAS	135.5	C_{in}, 99%; T, 25 °C	35
		92.4	C_{in}, 99%; T, 75 °C	
MCM-41	TEPA	211	C_{in}, 99%; T, 75 °C	31
MCM-48	APTS	50	C_{in}, 5%; T, 25 °C	34
hexagonal mesoporous silica	DT	59	C_{in}, 90%; T, 20 °C	20

APTS, 3-aminopropyl-triethoxysilane; DT, diethylenetriamine[propyl(silyl)]; EDA, *N*-[3-(trimethoxysilyl)propyl]ethylenediamine; HAS, hyperbranched aminosilica; PEI, polyethylenimine; TA, *N*-[3-(trimethoxysilyl)propyl]diethylenetriamine; TEPA, tetraethylenepentamine.

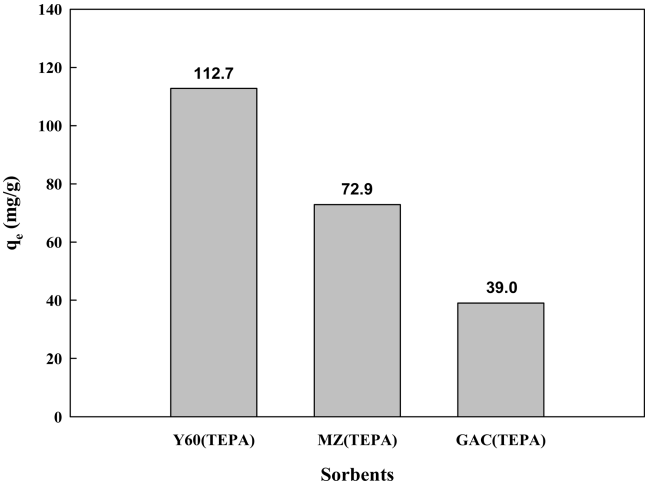

Figure 9. Comparisons of 15% CO_2 adsorption on TEPA-modified Y60, MZ, and GAC at 60 °C.

Second, the amine groups can also directly react with CO_2 and H_2O to form bicarbonate ion (HCO_3^-), as shown in reactions 6 and 7.[22]

$$CO_2 + RNH_2 + H_2O \leftrightarrow RNH_3^+ + HCO_3^- \quad (6)$$

$$CO_2 + R_2NH + H_2O \leftrightarrow R_2NH_2^+ + HCO_3^- \quad (7)$$

However, a further increase in the water vapor of air stream lead to the decrease in the CO_2 adsorption capacity. This might be explained by the competitive adsorption between CO_2 and H_2O at the same adsorption sites. It was indicated in the literature for amine functionalized MCM-41 materials that, when pre-exposed to moisture, the H_2O molecule will be absorbed and, thus, the CO_2 adsorption capacity could not be enhanced.[38]

Figure 9 presents the q_e of 15% CO_2 adsorption on Y60-(TEPA), MZ(TEPA), and GAC(TEPA) at 60 °C. It is seen that Y60(TEPA) has approximately 1.55 times the q_e of MZ(TEPA) and triple the q_e of GAC(TEPA), reflecting that Y60(TEPA) is an efficient sorbent for CO_2 capture from gas streams.

The comparisons of q_e via various raw and modified silica sorbents are given in Table 1. It is noted that the q_e of these sorbents can usually be enhanced after the modification by various kinds of grafting agents. Under similar conditions, Y60(TEPA) has good performance of CO_2 adsorption at 60 °C as compared to many other types of silica sorbents documented in the literature.

Isosteric Heat of Adsorption. The isosteric heat of adsorption (Q_{st}), which is defined as the difference between the activation energy for adsorption and desorption, represents the strength of the adsorbate−adsorbent interaction.[39] Quantification of Q_{st} is very important for kinetic studies of the adsorption process because the heat released upon adsorption is partially adsorbed on sorbents, which causes a rise in the sorbent temperature and thus slows the rate of adsorption.[40] The Q_{st} (kJ/mol) for the CO_2 adsorption on Y60(TEPA) at a given q_e was calculated from the Clausius−Clapeyron equation as[41]

$$\left(\frac{\partial(\ln P_{CO_2})}{\partial(1/T)}\right)_{q_e} = \frac{Q_{st}}{R} \quad (8)$$

where P_{CO_2} is the CO_2 partial pressure (Pa), T is the absolute temperature (K), and R is the universal gas constant (8.314 J mol^{-1} K^{-1}). For a given q_e, the C_{in} at multiple temperatures was obtained from Figure 6 and was subsequently converted to P_{CO_2}. The average Q_{st} of Y60(TEPA) at 30−60 °C for constant q_e of 70−110 mg/g (in 10 mg/g increments) was then determined from the slopes of the straight lines after plotting ln P_{CO_2} against $1/T$, as shown in Figure 10, and the results are given in Table 2. It is noted that the Q_{st} values were all positive, showing the endothermic nature of the adsorption process in 30−60 °C. The explanation is provided in the discussion of adsorption isotherms of CO_2 on Y60(TEPA). The Q_{st} tended to be less positive with a rise in surface loading (q_e), indicating a decrease in the strength of the CO_2−Y60(TEPA) interaction with surface loading. The Q_{st} was 27.6−46.97 kJ/mol, which was higher than that for a physical interaction but lower than that for a strong chemical interaction.

Cyclic CO_2 Adsorption. The optimum temperature and time for thermal regeneration of spent Y60(TEPA) must be determined before cyclic CO_2 adsorption. Figure 11 shows the CO_2 adsorption indexes of Y60(TEPA) at multiple desorption temperatures and times. The adsorption index

(38) Franchi, R. S.; Harlick, P. J. E.; Sayari, A. *Ind. Eng. Chem. Res.* **2005**, *44* (21), 8007–8013.

(39) Szekely, J.; Evans, J. W.; Sohn, H. Y. *Gas−Solid Reaction*; Academic: New York, 1976.

(40) Agnihotri, S.; Rood, M. J.; Rostam-Abadi, M. *Carbon* **2005**, *43* (11), 2379–2388.

(41) Ebbing, D. D.; Gammon, S. D. *General Chemistry*, 6th ed.; Houghton: Boston, MA, 1999.

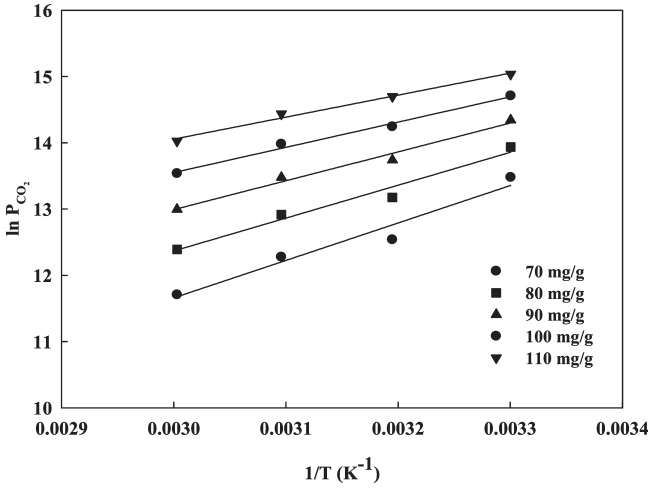

Figure 10. Regression lines of ln P_{CO_2} versus $1/T$ under various q_e.

Table 2. Isosteric Heats of 15% CO_2 Adsorption on Y60(TEPA)

	Q_{st} (kJ/mol)	
q_e (mg/g)	30−60 °C	r^2
70	46.97	0.990
80	41.25	0.990
90	36.20	0.982
100	31.68	0.971
110	27.60	0.957
average	36.74	

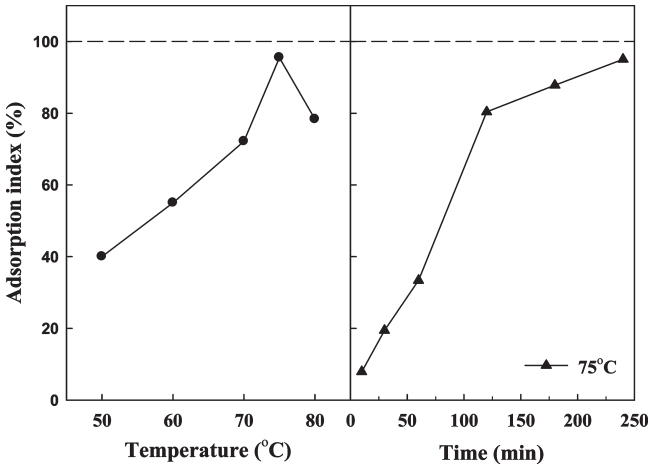

Figure 11. Effects of the desorption condition on the AI of CO_2: (a) desorption temperature and (b) desorption time.

(abbreviated as AI, %) was calculated on the basis of the percentage ratio of the adsorption capacity of the regenerated sorbents to the virgin one; thus, 100% AI indicates that the sorbent is not deteriorated at all. It is seen that the AI after 360 min of operation increased with the desorption temperature at 50−75 °C and reached 96% at 75 °C. As the desorption temperature further increased to 80 °C, the AI decreased to 79%. Thus, the desorption temperature of 75 °C was selected to determine the optimum desorption time. The AI also increased with the desorption time and reached 95% after 240 min of operation. Therefore, the desorption condition of 75 °C for 240 min was selected in the cyclic CO_2 adsorption.

Figure 12 shows the q_e and the AI of Y60(TEPA) at various cycles of adsorption and regeneration (n). It is seen

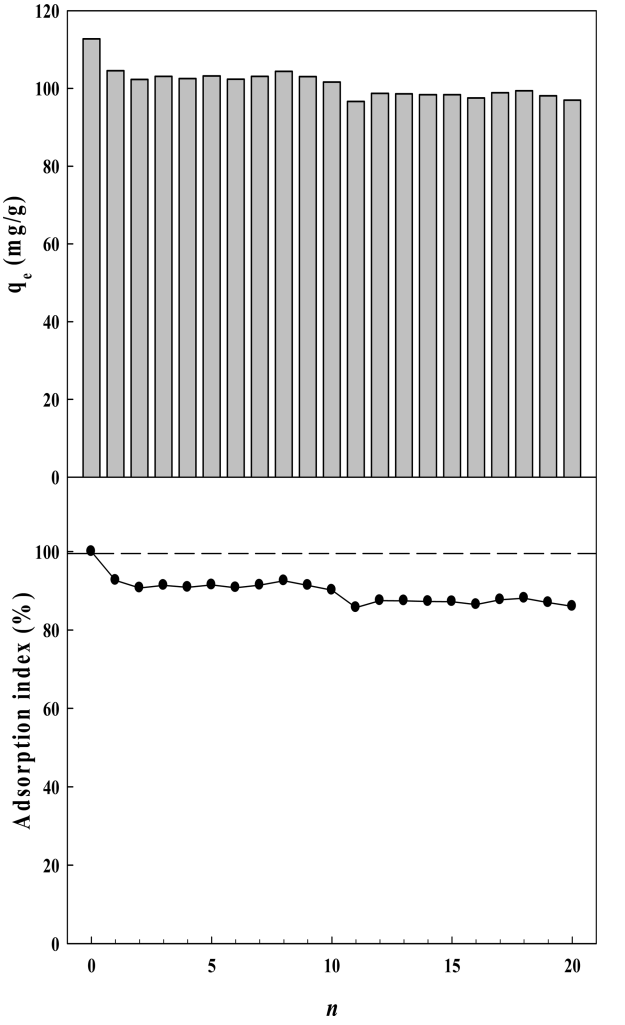

Figure 12. Cyclic CO_2 adsorption on Y60(TEPA).

that the q_e decreased from 114 to 106 mg/g, while the AI decreased from 100 to 93%, after the first cycle of operation, suggesting that most CO_2 molecules can be effectively desorbed from the surface of Y60(TEPA) at 75 °C for 240 min. However, the q_e reached stablity and showed only 3% attrition during the following 19 cycles of operation. This reflects that Y60(TEPA) can be employed in the prolonged cyclic CO_2 operation via a simple temperature swing operation.

Stability of Regenerated Y60(TEPA). The crystal phase, the thermogravimetric analysis, and the surface functional groups of Y60(TEPA) after 20 cycles of adsorption and regeneration are also presented in Figures 2−4, respectively. It is observed that the XRD pattern, the TGA and DTG profiles, and the IR spectrum of regenerated Y60-(TEPA) display similar results to those of virgin Y60-(TEPA). This reflects that the physicochemical properties of Y60(TEPA) were preserved during 20 cycles of operation.

It is apparent from the foregoing results that Y60(TEPA) not only displays high adsorption capacity of CO_2 but also shows a stable performance in the prolonged cyclic operation. The employed temperature for regeneration of spent Y60(TEPA) is also low (75 °C). These advantages suggest that Y60(TEPA) is a promising sorbent for CO_2 capture from flue gas.

Conclusions

Y60(TEPA) was selected as a sorbent to study adsorption/desorption behaviors of CO_2 from gas streams. The surface nature of Y60 was changed after the modification, which makes Y60(TETA) adsorb a significant amount of CO_2 gases. The CO_2 adsorption capacity of Y60(TEPA) increased with the temperature at 30−60 °C but decreased with the temperature at 60−70 °C. The CO_2 adsorption capacity of Y60(TEPA) was greatly influenced by the presence of water vapor and reached as high as 4.27 mmol/g at a water vapor of 7%. The mechanism of CO_2 adsorption on Y60 is entirely a physical interaction but appears mainly attributable to a chemical interaction after the TEPA modification. Y60(TEPA) has a good adsorption performance compared to TEPA-modified MZ and GAC conducted in this study or many other types of silica sorbents reported in the literature. The adsorption capacities and physicochemical properties of Y60(TEPA) were preserved after 20 cycles of adsorption and regeneration. This suggests that Y60(TEPA) can be employed in the prolonged cyclic CO_2 adsorption. Y60(TEPA) is thus possibly a cost-effective sorbent for CO_2 capture from flue gases.

Acknowledgment. The authors acknowledge support from the National Chung Hsing University, Taiwan, under plans to develop world-class universities and top-notch research centers.